Research article

Endoplasmic reticulum localization of phosphoinositide specific phospholipase C enzymes in U73122 cultured human osteoblasts

Matteo Corradini, Marta Checchi, Marzia Ferretti, Francesco Cavani, Carla Palumbo and Vincenza Rita Lo Vasco*

Section of Human Morphology, Department of Biomedical, Metabolic and Neural Sciences, University of Modena and Reggio Emilia, Modena, Italy

* **Correspondence:** Email: ritalovasco@hotmail.it; Tel: +390594224804.

Abstract: Different signal transduction pathways contribute to the differentiation and metabolic activities of osteoblasts, with special regard to the calcium-related pathway of phosphoinositide specific phospholipase C (PLC) enzyme family. PLC enzymes were demonstrated to be involved in the differentiation of osteoblasts and differently localize in the nucleus, cytoplasm or both depending on the isoform. The amino-steroid molecule U-73122 inhibits the enzymes belonging to the PLC family. In addition to the temporary block of the enzymatic activity, U-73122 promotes off-target effects, including modulation of the expression of selected *PLC* genes and different localization of PLC enzymes, depending on the cell line, in different cell lines.

In order to evaluate possible off-target effects of the molecule in human osteoblasts, we investigated the expression of *PLC* genes and the localization of PLC enzymes in cultured human osteoblasts (hOBs) in the presence of low dose U-73122.

Our results confirm that all *PLC* genes are transcribed in hOBs, that probably splicing variants of selected *PLC* genes are expressed and that all PLC enzymes are present in hOBs, except for PLC δ3 in quiescent hOBs at seeding. Our results confirm literature data excluding toxicity of U-73122 on cell survival. Our results indicate that U-73122 did not significantly affect the transcription of *PLC* genes. It acts upon the localization of PLC enzymes, as PLC enzymes are detected in cell protrusions or pseudopodia-like structures, at the nuclear or the plasma membrane, in membrane ruffles and/or in the endoplasmic reticulum.

Keywords: phospholipase C; phosphoinositide; endoplasmic reticulum; human osteoblast; U-73122

1. Introduction

The bone tissue is one of the most dynamic in the body, continuously undergoing remodeling, which requires the activity of the bone cells [1]. Homeostasis in the bone is strictly related to osteoblasts and osteoclasts, which must act to balance the activities. Osteoblasts are mononucleated cells which primarily produce and maintain the bone mass, also acting in bone injury repair [2,3]. Actually, a limited number of therapeutic agents are available to promote osteogenesis, addressed both to stimulate the activity of osteoblasts and to limit the activity of osteoclasts [4,5]. Different signal transduction pathways contribute to the differentiation and metabolic activities of osteoblasts, with special regard to calcium-related pathways. Knowledge of the signal transduction network acting in osteoblasts might represent the starting point for the modulation of bone remodeling and widen the panel of therapeutic agents, with special attention to the calcium-related pathways.

The concentration of calcium plays a critical role in bone remodeling, thus affecting the differentiation and proliferation of osteoblasts. G protein-coupled receptors (GPCRs) act regulating osteoblasts' activities *via* a number of different pathways [6], including the pathway of Phosphoinositide (PI)-specific Phospholipase C (PLC), involved in calcium metabolism [7–11].

We previously identified the panel of expression and the localization of PLC enzymes in human osteoblasts (hOBs), in differentiating hOBs and in inflammatory stimulated hOBs [12], confirming that PLC enzymes are present in osteoblasts and differently localize depending on the culture conditions [12].

The family of PLC enzymes belongs to the PI signal transduction pathway, which plays a pivotal role in a variety of cell functions [13–17]. PLC basically cleaves the polar head group of Phosphatidylinositol 4,5-bisphosphate (PIP2), producing both inositol trisphosphate (IP3) and diacylglycerol (DAG) [13]. Due to its water-solubility, IP3 diffuses to the cytoplasm, then binds IP3-gated calcium channels in the endoplasmic reticulum (ER) and induces release of calcium [13–15]. DAG can be cleaved into arachidonic acid [16], involved in the inflammatory response, or can activate the protein kinases C (PKCs) [13,15]. In addition to this basic function that all PLCs share, each enzyme is involved in different signaling networks [17,18].

Mammalian PLC enzymes were grouped into six sub-families, depending on slight structural and functional differences: β (1–4), γ (1–2), δ (1, 3, 4), ε, ζ, and η (1–2) [17]. Alternative splicing variants were described for most human PLC enzymes [19–23]. Each cell type bears a specific panel of PLC enzymes [24–29], and the sub-cellular distribution can modify the activity of PLC enzymes, suggesting specific roles for each enzyme beside the cleavage of PIP2 [30–32].

The panel of expression and the localization of PLCs differ in pathologic cells compared to normal controls depending on the culture conditions. The panel of PLCs can be modified by specific stimuli [33–37] or by use of specific inhibitors [28,38,39]. PLC enzymes were also recently described in extracellular vesicles (EVs), suggesting a possible role in extracellular signaling [40].

Inhibition of the PLC pathway offers insights to define the role of PLCs in the signaling of intracellular calcium concentration. It is actually considered an indirect tool to investigate involvement of PLCs in signal transduction networks and in cell growth/viability and to analyze the cross-talk among PLC enzymes in the cell [39,41].

U-73122 (1-[6-[[17β-3-methoxyestra-1,3,5(10)-trien-17-yl]amino]exyl]-1H-pyrrole-2,5-dione) was developed about 20 years ago as a specific inhibitor for PLC enzymes [42]. U73122, an amphiphilic alkylating agent and aminosteroid homologue of the thiol reagent N-ethylmaleimide (NEM),

is the most commonly used inhibitor of PLC enzymes. Controversial evidence suggested that PLC γ2 is not inhibited by U-73122 [43]. U-73122 acts by inhibiting the hydrolysis of PIP2 to IP3, thus leading to free cytosolic calcium reduction. The inhibition of the enzymatic activity of the PLC pathway following U-73122 treatment probably acts at the G-protein coupling level [44].

Recent evidence suggested that U-73122 might also act upon the transcription of selected *PLC* genes [38,39]. In MG-63 human osteosarcoma cell line, U-73122 induced a rearrangement of the panel of expression of the *PLC* genes after 1, 3, 6 and 24 hours [39].

Due to the numerous roles of PLCs, the effect of U-73122 upon transcription could modulate several activities involving PLC enzymes, including cell cycle control and apoptosis. As recently demonstrated, the intracellular distribution of PLC might be compartmentalized and related to different functions, including inclusion in vesicles (12, 40) or in protrusions (29, 37). The aim of the present study is to evaluate whether U-73122 acts upon the transcription of PLC genes and/or upon the intracellular localization of PLC enzymes also in osteoblasts.

In the present experiments, we analyzed the expression of *PLC* genes and the localization of PLC enzymes in hOBs cultured in the presence of U-73122 compared to untreated hOBs. Notably, the U-73122 molecule is not water soluble and needs to be dissolved in dimethyl sulfoxide (DMSO), an amphipathic dipolar aprotic molecule. We therefore cultured hOBs also in the presence of DMSO, to distinguish effects of U73122 in DMSO and DMSO itself upon cell cultures.

2. Materials and methods

2.1. Cell culture

HOBs were obtained from the American Type Culture Collection (ATCC, Rockville, MD, USA) and were characterized using antibodies against Osteocalcin, Alkaline Phosphatase, RUNX2, DMP1 and MEPE (data not shown). Frozen cells were thawed and cultured for 3 days. The initial seeding number of cells was 1×10^6 for each experiment. Cells were matured in T25 culture flasks for molecular biology experiments or upon 2 cm^2 coverslips in 24-multiwell plates for fluorescent immunocytochemistry under sub-confluent or confluent conditions. In either culture, cells were maintained at 37 °C with 5% CO_2 in Alpha Minimum Essential Medium (MEM) (Sigma-Aldrich, Steinheim, Germany), supplemented with 10% fetal bovine serum (GIBCO), penicillin (100 μg/ml) and streptomycin (100 U/ml) (Sigma-Aldrich). To maintain cultures, cells were split 1: 15 every 3 days. Cells were cultured in the following conditions: Control untreated cultures were maintained in culture medium, control cultures were maintained in medium added with DMSO 10 μM, treated cells were cultured in culture medium with added DMSO and U73122 10 μM. In cultured HOBs, reagent for molecular biology (see below) was added, or cells were fixed for immunocytochemistry analyses at the following time points: 0, 1, 2 and 7 days. For fluorescence immunocytochemistry experiments, cells were fixed at the following time points: 0, 2 and 3 days.

In all the indicated experimental conditions, HOBs were counted using a Neubauer hemocytometer (Weber Scientific International Ltd., Middlesex, UK), and morphology was observed using a Nikon optic microscope.

2.2. Molecular biology

Total RNA was isolated from samples by using TRIzol reagent (Invitrogen) following the manufacturer's instructions. The obtained RNA was quantitated by the UV absorption ratio 260: 280 nm by using a Nanodrop spectrophotometer (Thermo Scientific, Waltham, MA, USA), and 1 μg of total RNA was reverse transcribed by High-Capacity cDNA (r) Transcription Kit (ThermoFisher Scientific), according to the manufacturer's instructions. GoTaq(R) Colorless Master Mix (Promega, Madison, WI, USA) was used to amplify the obtained cDNA. The following primer pairs (DBA, Segrate, Italy) were used: *PLCB1* (OMIM *607120) forward (f) 5'-AGCTCTCAGAACAAGCCTCCAACA-3', reverse (r) 5'-ATCA TCGTCGTCGTCACTTTCCGT-3'; *PLCB2* (OMIM *604114) (f) 5'-AAGGTGAAGGCCTATCTGAGCCAA-3', (r) 5'-CTTGGCAAACTTCCCAAAGCGAGT-3'; *PLCB3* (OMIM *600230) (f) 5'-TATCTTCTTGGACC TGCTGACCGT-3', (r) 5'-TGTGCCCTCATCTGTAGTTGG CTT-3'; *PLCB4* (OMIM *600810) (f) 5'-GCA CAGCACACAAAGGAATGGTCA-3', (r) 5'-CGCATTT CCTTGCTTTCCCTGTCA-3'; *PLCG1* (OMIM *172420) (f) 5'-TCTACCTGGAGGACCCTGTGAA-3', (r) 5'-CCAGAAAGAGAGCGTGTAGTCG-3'; *PLCG2* (OMIM *600220) (f) 5'-AGTACATGCAGAT GAATCACGC-3', (r) 5'-ACCTGAATCCTGATTTGAC TGC-3'; *PLCD1* (OMIM *602142) (f) 5'-CTGAGCGTGTGGTTCCAGC-3', (r) 5'-CAGGCCCTCG GACTGGT-3'; *PLCD3* (OMIM *608795) (f) 5'-CCAGAACCACTCTCAGCATCCA-3', (r) 5'-GCCA TTG TTGAGCACGTAGTCAG-3'; *PLCD4* (OMIM *605939) (f) 5'-AGACACGTCCCAGTCTGGAACC-3'r 5'-CTGCTTCCTCTTCCTCATATTC-3'; *PLCE* (OMIM *608414) (f) 5'-GGGGCCACGGTCATCCAC-3', (r) 5'-GGGCCTTCATACCGTCCATCCTC-3'; *PLCH1* (OMIM *612835) (f) 5'-CTTTGGTTCGGTTCCT TGTGTGG-3', (r) 5'-GGATGCTTCTGTCAGTCCTTCC-3'; *PLCH2* (OMIM *612836) (f) 5'-GAAACT GGCCTCCAAACACTGCCCGCCG-3', (r) 5'-GTCTTGTTGG AGATGCACGTGCCCCTTGC-3'; *GAPDH* (OMIM * 138400) (f) 5'-CGAGATCCCTCCAAAATCAA-3'; (r) 5'-GTCTTCTGGGTGGCAGTGAT-3'. The specificity of the primers was verified by searching in the NCBI database for possible homology to cDNAs of unrelated proteins. The supplied reagents were mixed in a PCR tube with 0.2 mM primer pairs and 3–5 μl template cDNA, following the manufacturer's instructions, to 30 μl final volume. The amplification started with an initial denaturation step at 94 °C for 2 min and was followed by 30 cycles consisting of denaturation (30 s) at 95 °C, annealing (30 s) at the appropriate temperature for each primer pair and extension (1 min) at 72 °C. The PCR products were analyzed by electrophoresis of 1.5% TAE agarose gel. Gels were previously stained with GelRed® Nucleic Acid Gel Stain (Biotium Inc, Fremont, CA). Chemidoc Imaging System (Bio-Rad, Hercules, CA) was used for gel documentation and image acquisition. Optical densities were normalized to the RNA transcript of glyceraldehyde-3-phosphate dehydrogenase human gene (*GAPDH*; OMIM * 38400), a typical reference constitutive transcript. To exclude possible DNA contamination during the RT-PCR, RNA samples were amplified by PCR without reverse transcription. No band was observed, excluding DNA contamination during the RNA preparation procedure (data not shown).

2.3. PLCs localization

Cells grown upon coverslips were washed three times with PBS, fixed with 4% paraformaldehyde (PFA) in phosphate buffer saline (PBS) for 10 min at 4 °C and washed three times with PBS. Cells

were incubated at 4 °C overnight in a humidified chamber with appropriate primary antibodies diluted (1: 100) in PBS. The primary mouse anti-human PLC antibodies against enzymes belonging to the PLC β, PLC γ and PLC δ sub-families (Santa Cruz Biotechnology, Santa Cruz, CA) were detected with the appropriate fluorescent dye conjugated anti-mouse secondary antibodies (Bethyl Laboratories, Montgomery, TX). The primary rabbit anti-human PLC antibodies against enzymes belonging to PLC ε and η sub-families (Invitrogen, Thermofisher Scientific) were detected with the appropriate fluorescent dye conjugated secondary antibodies (Thermoscientific, Thermofisher Scientific). Cover-slips were incubated with the specific secondary antibody (1: 200) for 1 h at room temperature (RT) in the dark. Cells were washed twice with PBS for 5 min and then counterstained with 4',6-diamidino-2-phenylindole (DAPI) fluorescent staining for 20 min at RT in the dark. After two washes in PBS for 5 min each, the slides were visualized, and images were captured with a Nikon fluorescence microscope equipped with NIS Elements software (Nikon Imaging Japan Inc, Tokyo).

2.4. Endoplasmic reticulum localization

Cells grown upon coverslips were washed three times with PBS, fixed with 4% paraformaldehyde (PFA) in phosphate buffer saline (PBS) for 10 min at 4 °C and washed three times with PBS. Cells were incubated at 4 °C overnight with appropriate primary antibodies diluted (1:100) in PBS. One primary mouse anti-human PLC antibody addressed against each PLC β1, PLC β2, PLC β4, PLC γ2, PLC δ1, PLC δ3, PLC δ4 (Santa Cruz Biotechnology, Santa Cruz, CA) or primary rabbit anti-human addressed to PLC ε (Thermoscientific) was incubated overnight at 4 °C in a humidified chamber with primary goat anti human calnexin (Abcam, Cambridge, UK). After several PBS washes, coverslips were incubated with the appropriate fluorescent dye conjugated anti-mouse (Bethyl Laboratories, Montgomery, TX) or anti-goat (Thermoscientific) secondary antibodies, 1 hour at RT in the dark. Coverslips were counterstained with DAPI fluorescent staining for 20 min at RT in the dark. Images were visualized and captured with a Nikon fluorescence microscope equipped with NIS Elements software (Nikon Imaging Japan Inc, Tokyo).

3. Results

3.1. Cell culture

The cell growth did not significantly differ in the 3 analyzed cell populations during a 14 day culture interval (Table 1, Figure 1). Statistical analysis of the data was conducted using Student's t test, ANOVA and Shapiro Wilk tests, and it did not identify any significant difference (p value > 0.05) (Figure 1, Table 1).

Table 1. Growth data of cultured cells. Ctrl: control cells; DMSO: cells grown in the presence of DMSO; INHU: cells grown in the presence of U-73122 dissolved in DMSO. Viable cells' numbers were counted before adding molecules to the cultures (G0: seeding day) and after 1 (G1), 3 (G3), 7 (G7) and 14 (G14) days.

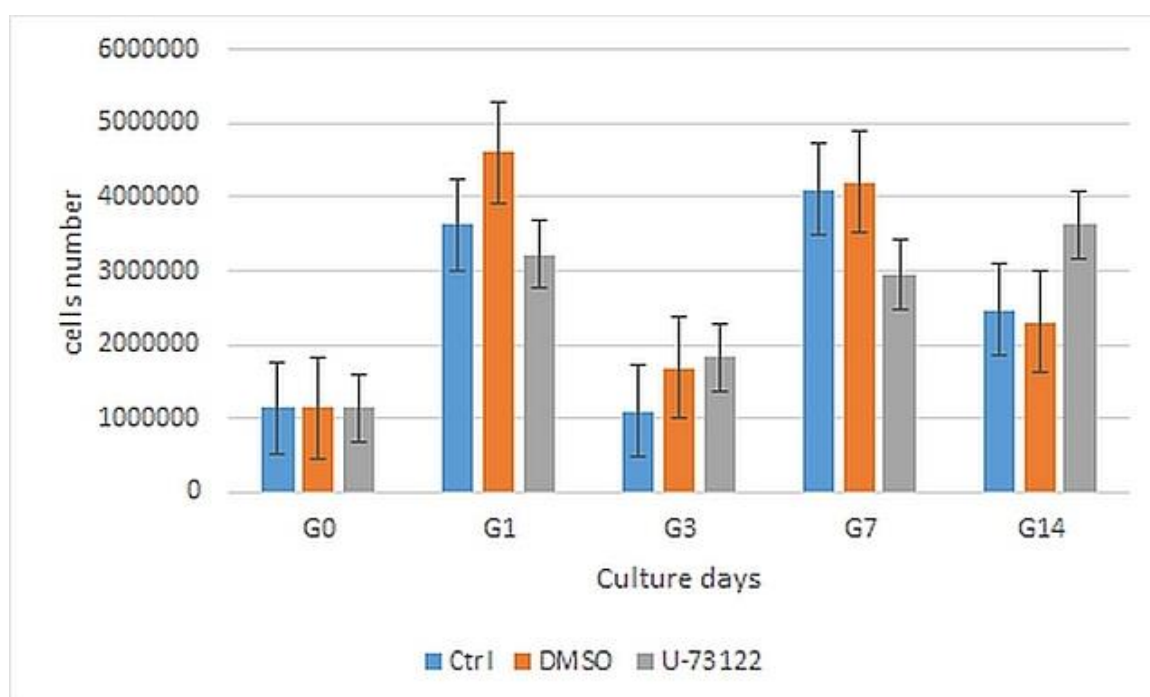|	Ctrl	DMSO	INHU
G0	1146667	1146667	1146667
G1	3633333	4606667	3222667
G3	1100000	1683333	1826667
G7	4106667	4193333	2946333
G14	2470000	2310000	3630000

Figure 1. Histogram of the cell growth data. Histogram of the cell growth data in Table 1 with error bars [Ctrl: control cells; DMSO: cells grown in the presence of DMSO; U-73122: cells grown in the presence of U-73122 dissolved in DMSO before adding molecules to the cultures (G0) and after 1 (G1), 3 (G3), 7 (G7) and 14 (G14) days].

3.2. Molecular biology

The transcripts of all PLC genes were detected in all the experimental conditions and in the considered intervals, with the noTable exception of day G0, when PLC δ3 is not expressed, and PLC δ4 is very weakly expressed. In this case, we used the RT-PCR method, which is not a quantitative technique, and it is not possible to compare the concentrations of transcripts. However, selected bands have different intensities, suggesting that decreases/increases in transcripts' concentrations have occurred. PLC β1 was detected with a double band in U-73122 treated cells at G2. PLC γ1 was detected as a double band in treated cells at G1. PLC η2 was detected as a double band in all the experimental conditions (Figure 2).
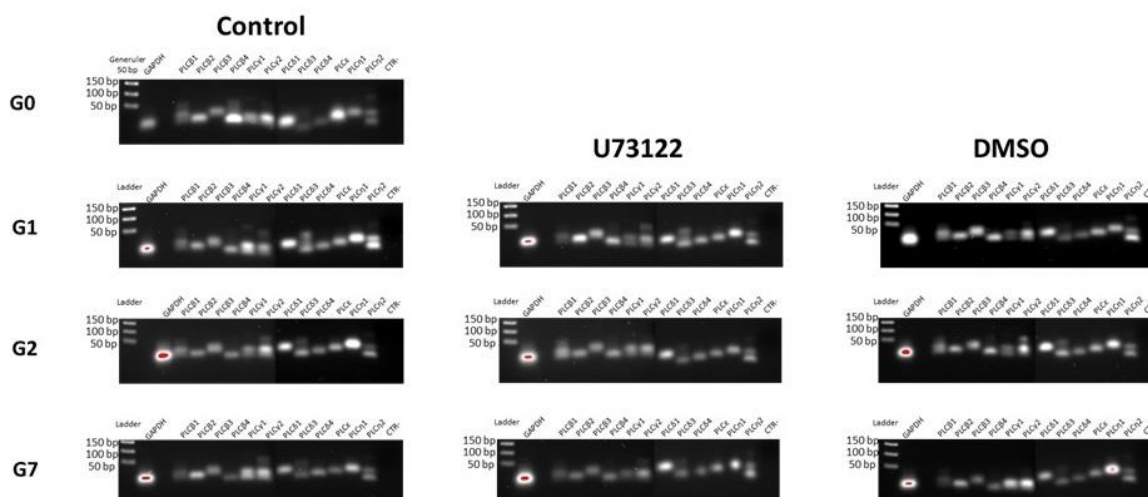
Figure 2. Gel electrophoresis of PCR results. PCR results. Agarose gel electrophoresis of PCR amplified reverse transcripts of *PLC* genes and of *GAPDH* gene as a positive control. See the left column for reference transcript length.

3.3. PLCs localization

3.3.1. Day 0

All PLCs were detected, except for PLC δ3 (Table 2). PLC β1, PLC β4 and PLC γ1 were weakly detected in the nucleus. PLC β2 was weakly detected both in the nucleus and in the cytoplasm (Figure 3). PLC β3, PLC δ4 and PLC ε were weakly detected both in the nucleus and in the perinuclear area of the cytoplasm. PLC γ2 was weakly detected in the cytoplasm (Table 2). PLC δ1 was detected in the nucleus and with punctate distribution in the perinuclear area of the cytoplasm. PLC η1 was detected in the nucleus, in the cytoplasm and in cell protrusions. PLC η2 was detected both in the nucleus and in the perinuclear area of the cytoplasm (Table 2).
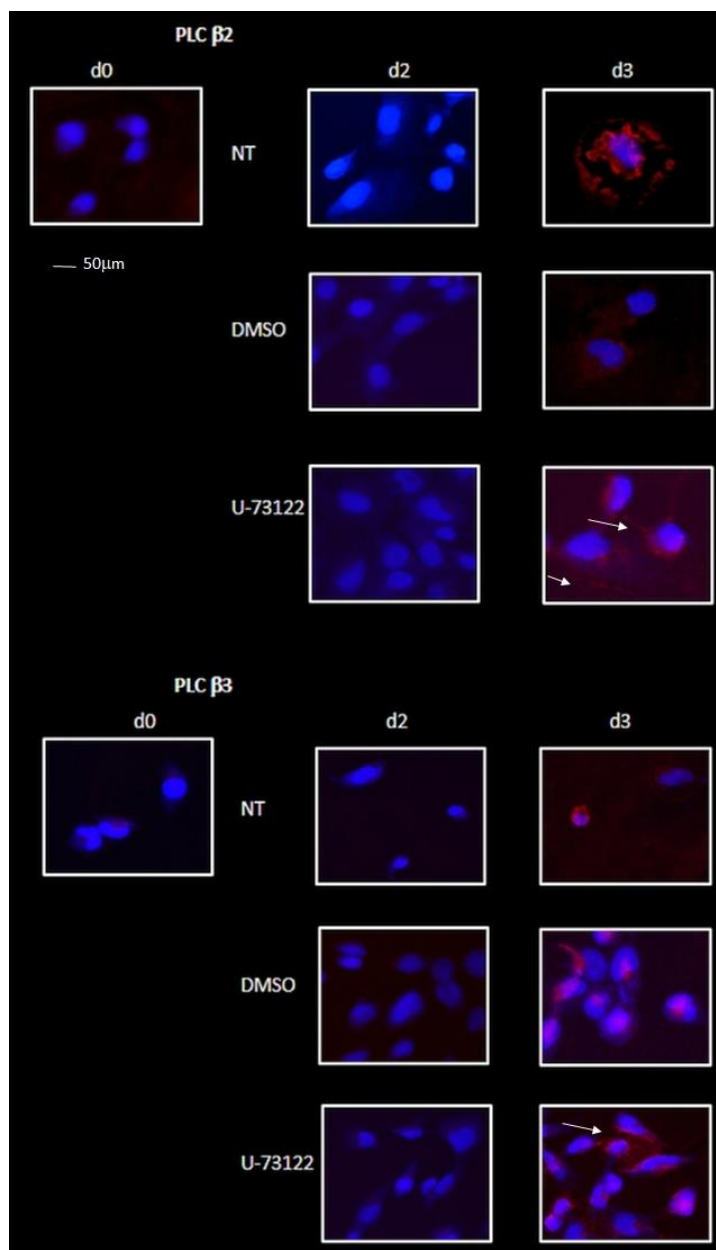
Figure 3. Fluorescence immunocytochemistry location of PLC β2 and PLC β3 (40X). Fluorescence immunocytochemistry. Intracellular localization of PLC β2 and PLC β3 (red). Nuclei counterstain with DAPI (blue). White arrows: PLCs in cell protrusions. [Caption 40X].

3.3.2.   Untreated control cells

All PLCs were detected at day 2, with all excepting PLC ε at day 3. PLC β1 was detected in the nucleus at days 2 and 3 and in the cytoplasm at day 2, where it was punctuate distributed at day 3. PLC β2 was detected both in the nucleus and in the perinuclear area of the cytoplasm at day 2 and exclusively in the cytoplasm at day 3 (Figure 3). PLC β3 was weakly detected both in the nucleus and in the perinuclear area of the cytoplasm at day 2 and detected exclusively in the cytoplasm at day 3

(Figure 3). PLC β4 was weakly detected in the nucleus and very weakly in the cytoplasm at days 2 and 3 (Table 2). PLC γ1 was weakly detected in the nucleus at day 2, well detected at the nuclear membrane at day 3 and well detected in the perinuclear area of the cytoplasm at days 2 and 3. PLC γ2 was weakly detected in the nucleus and punctuate in the perinuclear area of the cytoplasm at day 2, while at day 3 it was detected both in the nucleus and the cytoplasm. PLC δ1 was detected in the nucleus exclusively at day 2 and was detected in the perinuclear area of the cytoplasm at day 3 (Table 2). PLC δ3 was weakly detected both in the nucleus and in the cytoplasm at day 2 and in the cytoplasm and in cell protrusions at day 3. PLC δ4 was detected in the nucleus at days 2 and 3, in deposits in the perinuclear area of the cytoplasm at day 2 and diffuse in the cytoplasm and on the plasma membrane at day 3. PLC ε was weakly detected both in the nucleus and cytoplasm at day 2 and weakly detected in the cytoplasm at day 3. PLC η1 was detected in the nucleus, in cell protrusions and weakly detected in the cytoplasm at day 2, and at day 3 it was compartmentalized in the cytoplasm. PLC η2 was detected in the cytoplasm at day 2, but at day 3 compartmentalized distribution in the cytoplasm was observed. (Table 2).

3.3.3.   DMSO cultured cells

All PLCs were detected in the analyzed time intervals (Table 2). PLC β1 was weakly detected in the nucleus at day 2, where it was well detected at day 3, and weakly detected with punctuate distribution in the perinuclear area of the cytoplasm at days 2 and 3 (Table 2). PLC β2 was weakly detected both in the nucleus and punctuate in the perinuclear area of the cytoplasm at day 2 and at day 3 at the nuclear membrane and in the cytoplasm (Table 2, Figure 3). PLC β3 was detected in the nucleus at days 2 and 3 and punctuate in the cytoplasm at day 3 (Figure 3). PLC β4 was detected in the nucleus at days 2 and 3, although the signal was weaker at day 2; in the cytoplasm it was weakly detected with punctuate distribution at day 2 and well detected punctuate in the whole cytoplasm at day 3 (Table 2). PLC γ1 was weakly detected in the nucleus at day 2, and the intranuclear signal was stronger at day 3. PLC γ2 was weakly detected in the nucleus at days 2 and 3 and punctuate in the perinuclear area of the cytoplasm at day 2, while at day 3 it was weakly diffuse in the whole cytoplasm (Table 2). PLC δ1 was weakly detected both in the nucleus and punctuate in the perinuclear area of the cytoplasm at day 2 and well detected both in the nucleus and cytoplasm at day 3. PLC δ3 was weakly detected in the nucleus at day 2 and at day 3 it was detected well in the nucleus and weakly in the cytoplasm with punctuate distribution. PLC δ4 was weakly detected both in the nucleus and the cytoplasm at days 2 and 3, showing punctuate cytoplasmic distribution at day 3 (Table 2). PLC ε was detected in the cytoplasm and in cell protrusions at day 2 and in the nucleus and compartmentalized in the cytoplasm at day 3. PLC η1 was detected in the cytoplasm and at the plasma membrane at day 2 and in the nucleus, cytoplasm and in cell protrusions at day 3. PLC η2 was detected at the nuclear membrane and in the cytoplasm at day 2 and in the nucleus, cytoplasm and in cell protrusions at day 3 (Table 2).

3.3.4. U-73122 in DMSO cultured cells

Table 2. Results of fluorescence immunocytochemistry experiments for the intra-cellular localization of PLC enzymes. N = intranuclear; C: cytoplasmic; pn = perinuclear cytoplasmic distribution; Cpns = subtle perinuclear cytoplasmic halo; Cpnw = wide perinuclear cytoplasmic halo; dep = deposits; Pr = cell protrusions; punct = punctuate distribution (vesicles); pM = plasma membrane; nM = nuclear membrane; comp = compartmentalized position in the cell; fil = filamentous distribution; pspod = pseudopodia-like structures; Mru = membrane ruffles. G0: seeding day. G2: 2 days culture.

	PLC β1	PLC β2	PLC β3	PLC β4	PLC γ1	PLC γ2	PLC δ1	PLC δ3	PLC δ4	PLC ε	PLC η1	PLC η2
G0	-/+N -/+C	-/+N -/+Cpn	-/+N	-/+N	-/+N	-/+ C	N Cpn punct	-	-/+N -/+Cpn	-/+N - /+Cpn	N C Pr	N Cpn
G2												
G2 UT	N C	N Cpn	-/+ N -/+ C	--/+N -/+C	-/+N Cpn	-/+Ns Cpn punct	N Cpn	-/+N -/+C	N Cpn dep	-/+N -/+C	N -/+C Pr	C
G2 dmso	-/+N -/+Cpn punct	-/+N -/+Cpn punct	N	-/+N -/+Cpn punct	--/+N	-/+N -/+ Cpn punct	-/+N -/+ Cpn punct	-/+N	-/+N -/+ Cpn punct	C Pr M	C	nM C
G2 INHU	--/+N -/+C	--/+N	N -/+Cpn	N -/+C	N - /+Cpn	N C	N Cpn	N -/+ Cpn punct	-/+N -/+Cpn	N dep C pM	N dep C	Nm N dep C Pr
G3												
G3 UT	N C punct	C	C	-/+N -/+C	nM - /+Cpn	N C	Cpn	C Pr pM	N C	-/+ C	C comp	C comp
G3 dmso	N -/+ Cpn punct	nM C	N C punct	N comp C punct	N	-/+N -/+C	N C	N -/+C punct	-/+N -/+C	N C comp	N C Pr	N C Pr
G3 INHU	N nM	N C Pr pspod Mru	C fil Pr pspod Mru	N Cpns	N C	N Cpn comp	N -/+C	-/+N Cpn	N Cpn	N C	N Cpnw	--/+ N

All PLCs were detected in the analyzed time intervals (Table 2). PLC β1 was weakly detected in the nucleus and the cytoplasm at day 2, and at day 3 it was evident exclusively in the nucleus, with a marked nuclear membrane signal. PLC β2 was weakly detected in the nucleus at day 2 and at day 3 in

the nucleus, in the cytoplasm and in cell protrusions, such as pseudopod-like structures and membrane ruffles (Figure 3). PLC β3 was detected in the nucleus and weakly in the perinuclear area of the cytoplasm at day 2 while filamentous in the cytoplasm and in cell protrusions, such as pseudopod-like structures and membrane ruffles, at day 3 (Table 2, Figure 3). PLC β4 was detected in the nucleus at days 2 and 3 and weakly detected in the cytoplasm at day 2, where it was located in the perinuclear area as a subtle halo at day 3. PLC γ1 was detected in the nucleus at days 2 and 3, weakly in the perinuclear area of the cytoplasm at day 2 and well diffused in the cytoplasm at day 3. PLC γ2 was detected in the nucleus at days 2 and 3, diffuse in the cytoplasm at day 2 and in the perinuclear area of the cytoplasm at day 3. PLC δ1 was detected in the nucleus at days 2 and 3, in the perinuclear area of the cytoplasm at day 2 and weakly in the cytoplasm at day 3 (Table 2). PLC δ3 was detected in the nucleus at day 2, with a weaker signal at day 3, and weakly detected in the perinuclear area of the cytoplasm with a punctuate distribution at day 2, where the signal was stronger at day 2, but the punctuate distribution was replaced by diffuse presence at day 3. PLC δ4 was detected in the nucleus and in the perinuclear area of the cytoplasm at days 2 and 3, with weaker signal at day 2. PLC ε was detected in deposits in the nucleus at day 2, diffuse in the nucleus at day 3, and in the cytoplasm at day 2 and 3. PLC η1 was detected in deposits in the nucleus at day 2 and diffuse in the nucleus at day 3, and it was detected diffuse in the cytoplasm at day 2. It was located in a perinuclear wide area of the cytoplasm at day 3, and it was also evident as a marked signal in the plasma membrane. It was detected in the cytoplasm and at the plasma membrane at day 2 and in the nucleus, cytoplasm and cell protrusions at day 3. PLC η2 was detected at the nuclear membrane, in deposits in the nucleus, in the cytoplasm and in cell protrusions at day 2 and weakly exclusively in the nucleus at day 3 (Table 2).

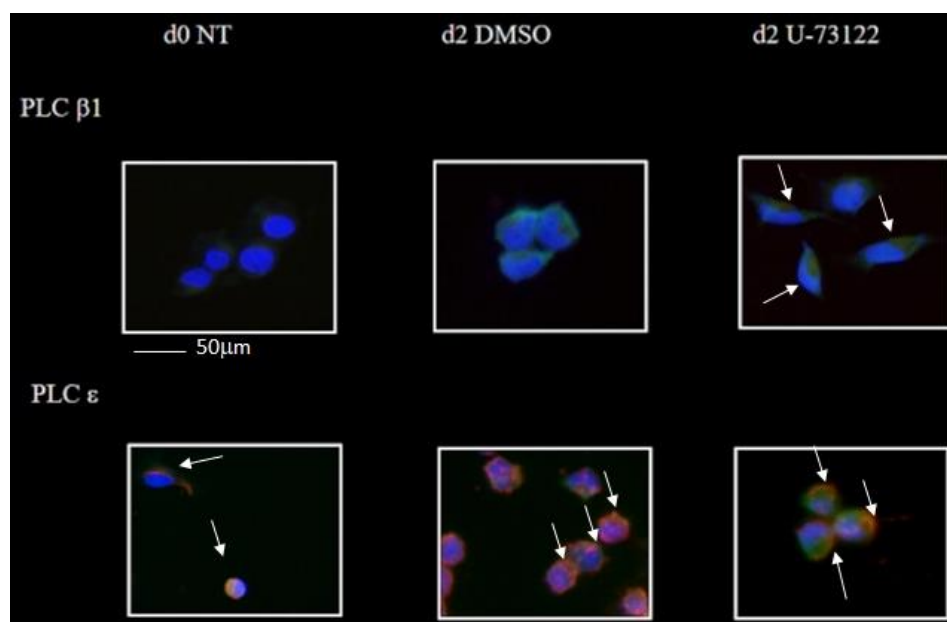### 3.4. Endoplasmic reticulum localization

Figure 4. Fluorescence immunocytochemistry location of PLC ε at the ER (40X). Double fluorescence immunocytochemistry. Localization of PLC ε (red) at the ER (Calnexin, green). Nuclei counterstain with DAPI (blue). White arrows: co-localization site. [Caption 40X].

The fluorescence double immunocytochemistry experiments conducted for selected PLCs we had detected with peculiar compartmentalized localization upon a side of the cytoplasm (resembling the position of the endoplasmic reticulum) confirmed the co-localization of some enzymes with calnexin (Table 3, Figure 4). In the seeded population (G0), PLC β1 and PLC ε co-localized with calnexin. In cells cultured 2 days in medium and DMSO, PLC γ2, PLC δ enzymes and PLC ε co-localized with calnexin. In cells cultured 2 days with the addition of inhibitor U73122 in DMSO, the following enzymes co-localized with calnexin: PLC β1, PLC γ2, PLC δ3 and PLC ε (Table 3, Figure 4).

Table 3. Fluorescence double immunocytochemistry experiments for the localization of PLC enzymes in the endoplasmic reticulum. - = no co-localization of a PLC enzyme with calnexin; + = co-localization of a PLC enzyme with calnexin. G0: seeding day. G2: 2 days culture.

G0		G2 DMSO	G2 INHU
+	PLC β1	-	+
	PLC β2	-	-
	PLC β4	-	-
	PLC γ2	+	+
	PLC δ1	+	-
	PLC δ3	+	+
	PLC δ4	+	-
+	PLC ε	+	+

4. Discussion

The metabolism of calcium plays a critical role in bone remodeling, also affecting the differentiation and proliferation of osteoblasts. Signal transduction pathways involved in calcium metabolism include the PLC family of enzymes. The present study aims to evaluate in human osteoblasts the possible off target effects of U-73122, which might affect both the transcription of *PLC* genes and the localization of PLC enzymes. Due the multiple roles of PLC enzymes [17], these off target effects might interact with cell cycle control, apoptosis and cytoskeleton dynamics.

We previously demonstrated the presence of all *PLC* genes' transcripts and defined the intracellular localization of PLC enzymes in osteoblasts, cultured under different conditions [12]. In this case, we cultured hOBs in the presence of U-73122 inhibitor of PLC's enzymatic activity. U-73122 seems to bear off target effects, including the modulation of the transcription of *PLC* genes [38,39]. We cultured human osteoblasts (hOBs) in the presence of low-dose U-73122 in order to evaluate possible effects upon both the transcription of *PLC* genes and the localization of PLC enzymes compared to untreated hOBs. The statistical analysis of the cell growth data showed no significant differences in the cell cultures treated with U-73122 compared to the untreated cell cultures or to cell cultures grown in the presence of DMSO. Our data confirm that DMSO and low-dose U-73122 do not affect cell growth and survival (Table 1).

The present results confirm the presence of transcripts from all *PLC* genes in hOBs. We observed double band transcripts for selected *PLC* genes, confirming the hypothesis that PLCs' splicing isoforms might exist in human osteoblasts, depending upon the culture conditions [12]. A double band transcript of *PLCG2* gene was visualized in untreated cells, at day 2 of DMSO cultures and after 1 day after U-73122

treatment. The transcript of *PLCH2* was visualized as a double band in all the experimental conditions (Figure 2), confirming previous report [12]. These observations require further investigation. Slight variations in the visualization of the transcripts of other *PLC* genes were observed. The intensity of selected bands seems to differ depending on the culture conditions. Visual observations were confirmed by normalizing the band intensities, referring to the housekeeping gene with the BioRad ImageLab program (data not shown). Quantitative analyses of transcripts from *PLC* genes will be required in order to confirm these supposed variations of the concentration of mRNA depending on U-73122 treatment.

Although in the present experiments U-73122 had no ON/OFF effect upon the transcription of *PLC* genes, it affected the localization of PLC enzymes (Table 2). The present results confirm previous data indicating the presence of most PLC enzymes in hOBs, both in the nucleus and cytoplasm [12], supporting the hypothesis that a nuclear cycle might exist for other PLC enzymes besides the well characterized PLC β1 nuclear cycle. Our data confirm the absence of PLC δ3 in quiescent hOBs at seeding (day 0 culture, after cell thawing) [12]. Our present results confirm the presence of selected PLC enzymes in intracellular vesicles (IVs), especially in cells cultured in the presence of DMSO. PLC enzymes were also detected in cell protrusions or pseudopodia-like structures, as previously described [12]. We presently observed selected PLC enzymes marking the nuclear or the plasma membrane and in membrane ruffles. Selected PLC enzymes localized in the ER, slightly differing depending on the culture conditions. Some PLC isoforms and observations deserve addressed comments.

The transcript of the *PLCB1* gene was visualized as a double band 2 days after treatment with U-73122. Imaging analyses demonstrated the presence of the PLC β1 enzyme both in the nucleus and the cytoplasm. Two splicing variants of *PLCB1* were reported [19]. PLC β1b is almost entirely nuclear, and PLC β1a was described also in the cytoplasm [19,45]. That might suggest that either splicing variant, PLC β1a or PLC β1b, acts in hOBs. The presence of double band transcript might indicate presence of transcripts of either variant. This observation will require further investigations in order to sequence the transcript of *PLCB1* and to localize the splicing variant PLC β1a and PLC β1b enzymes in the cell. In cultured hOBs, PLC β1 was initially slightly detected in the nucleus, and after 3 days culture it was in the nucleus and punctuate in the cytoplasm. In hOBs cultured with DMSO added to the medium, PLC β1 was early detected punctuate in the cytoplasm. Interestingly, in hOBs cultured in the presence of U-73122, PLC β1 was exclusively found in the nucleus, and at day 3 from treatment it was also marked at the nuclear membrane. Thus, the presence of U-73122 seems to prevent PLC β1 from moving to the cytoplasm. That might be related to the specific role played by PLC β1 in the differentiation of osteoblasts [46]. One might speculate that, as U-73122 blocks PLC enzymatic activity, probably in hOBs the pro-differentiating activity of PLC β1 is carried out in the cytoplasm. Finally, PLC β1 localizes in the ER at day 0 (seeding) and at day 2 in U-73122 treated hOBs but not in day 2 DMSO cultures. These observations demonstrated that the effects of DMSO alone and U-73122/DMSO upon hOB cultures differ.

Further interesting observations regard the effects of DMSO or U-73122/DMSO upon the localization of other PLC enzymes. In untreated cultured cells, selected PLC enzymes were initially detected in the nucleus or exclusively in the cytoplasm: PLC η2 at days 2 and 3 and PLC β2, PLC β3, PLC δ1, PLC δ3 and PLC η1 at day 3 of the culture. Apparently, the PLC enzymes move from the nucleus to the cytoplasm during the culture interval, although with different rapidity (Table 3). That is particularly evident for PLC β1, PLC β4 and PLC γ1 enzymes (Table 3). In untreated hOBs PLC ε was

slightly detected at days 0 and 2, and it was not detected at day 3 of culture, partially according to previous observations [12].

Adding DMSO to the seeding culture medium slightly modified the intracellular localization of PLC enzymes. DMSO is water soluble, commonly and widely used as a solvent for water-insoluble compounds, a cryoprotectant for cell storage, a vehicle for drug therapy and an inducer of multilineage differentiation of embryonic and adult progenitor cells, and it bears fusogenic properties [17–51]. DMSO acts as a differentiating agent, playing multiple roles both in cellular functions (e.g., metabolism and enzymatic activity) and cell growth by affecting cell cycle and apoptosis [52]. Despite the widespread use, side effects and mechanisms of action of DMSO are not fully clear. DMSO affects the organization and properties penetrating the cell membranes and acts in different roles in cellular functions. DMSO was demonstrated to induce differentiation in stem and endothelial cells [53]. Understanding the effects of DMSO on cells' membranes might allow better definition of experimental results when it is used, especially as a solvent. The toxicity of DMSO was reported, depending on the concentration [54,55].

All PLCs were detected in the nucleus during the whole culture interval, with the noTable exception of day 2, when PLC ε and PLC η1 were exclusively detected in the cytoplasm (Table 3). Following DMSO addition, PLC γ1 exclusively localized in the nucleus and not in the cytoplasm. Thus, adding DMSO seems to reduce the displacement of PLCs from the nucleus to the cytoplasm. That is particularly evident for the PLC γ1 enzyme, exclusively detected in the nucleus during the entire culture period. The enzymes belonging to the PLC η family were detected in cell protrusions, especially at day 3. According to literature data, our present results suggest that DMSO addition might improve the formation of IVs. In fact, selected PLC enzymes were punctuate distributed in the cytoplasm, such as all the enzymes belonging to PLC β and PLC δ families. PLC γ2 was punctuate distributed in the cytoplasm in both untreated and DMSO treated hOBs (Table 3).

Our present observations might fit with literature data reporting DMSO to increase the exocytosis of neurotransmitters [56]. DMSO treated cells showed faster release kinetics compared to untreated ones, suggesting that DMSO significantly affects the biochemistry and fluidity of the cell membrane, increasing exocytosis [56]. Three regimes of activity for DMSO were reported in single-component and cholesterol-containing lipid bilayers at increasing concentrations, including loosening, thinning and increased fluidity of the hydrophobic core followed by pores in the lipid bilayer [57–61]. The punctuate distribution of PLCs we here observed in DMSO treated hOBs probably indicate the presence of IVs and might be due to the effects of DMSO upon the cell membranes.

Treating hOB cultures with U-73122 promotes more effectively the nuclear presence of PLCs, thus reducing the translocation from the nucleus to the cytoplasm. All PLC enzymes were detected in the nuclei or in both the nucleus and cytoplasm, except for PLC β3. At day 3, the PLC β3 enzyme was detected in the cytoplasm with filamentous distribution, in cell protrusions and membrane ruffles (Figure 3). U-73122, the most archetypal inhibitor of PLC enzymes, inhibits calcium mobilization in a dose-dependent manner by PLC inhibition. U-73122 probably inhibits the PLC enzymes acting at G protein coupling level [44] and prevents the turnover of PI [62,63]. Lack of selectivity of PLC inhibition by U-73122 was described. In fact, U-73122 acts [64] upon different unrelated proteins [65–69]. Recent evidence suggests that U-73122 has different off-target effects, including the ability to modulate the expression of *PLC* genes and the localization of PLC enzymes in cultured cells [38–39].

We previously reported the transcripts panel of *PLC* genes and the sub-cellular distribution of PLC enzymes in MG-63 human osteoblast-like osteosarcoma cells [27,39] after adding 30 μM U-73122

to cell cultures. Based on this observation, we here used lower U-73122 (10 μM) concentrations in order to preserve the growth and survival rates of cultured hOBs. U-73122 reduced MG-63 cells growth and modified the transcription of selected PLC genes [39], with special regard to *PLCB1*. In the present experiments, the transcript of *PLCB1* was detected as a double band 2 days from U-73122 culture. Accordingly, PLC β1 was detected in the nucleus and at the nuclear membrane during the entire culture interval. Moreover, selected PLCs, namely, PLC ε and enzymes belonging to the PLC η family, were observed as deposits within the nucleus.

In hOBs after 3 days from the treatment with U-73122, PLC β2 and PLC β3 were located in pseudopodia-like structures and in membrane ruffles (Table 2, Figure 3).

This observation might pave the way to a possible role of PLC enzymes in the formation of cell protrusions, the inclusion in extra cellular vesicles (EVs) content or involvement in cell migration. In mammalian cells, the dynamic remodeling/reorganization of the cytoskeleton represents the basis for shape adaptation and migration [70,71].

Cell migration is central in a number of biological and pathological processes, such as metastasizing tumor spread. Migrating and spreading cells form flat, actin-supported, organelle-free regions, referred to as lamellipodia, and other features which may expand their attachment area [72]. Migration starts from acquisition of spatial asymmetry visible as polarized cell morphology. In cell migration, a multistep cycle occurs, first requiring extension of membrane protrusions, such as lamellipodia, and filopodia, at the cell lamella, the front and flat region of the motile cell missing organelles [73–81]. Lamellipodia can fail to establish stable adhesions, detaching from the substrate and retracting toward the cell body [82–85]. This retraction leads to the formation of membrane ruffles, sheet-like protrusions, emerging at the cell edge, moving centripetally and disappearing at the border between the cell lamella and the main cell body [86–88]. Despite the growing interest related to the possible involvement in tumor metastasis spreading, the structure and molecular composition of membrane ruffles and the signal transduction pathways recruited during their formation are still largely unknown.

By contrast with the behavior of Phosphatidylinositol (3,4,5)-trisphosphate (PIP3), the levels of PIP2 in the membrane ruffles forming macro-pinocytic cups increased compared to planar plasma membranes [88]. PIP2 levels in the membrane are the highest before macro-pinosome closure and decrease after [88]. Authors suggested that local control of PI levels acts crucially in the regulation of actin-binding proteins which effect changes in the membrane architecture [88]. Ruffles were described in osteoblasts on the cell rims, vanishing after a large adhesion area consolidates, resulting in a smooth apical plasma membrane surface. The presence of ruffles, differently localized in the cell, is usually associated with migration, receptor internalization and macropinocytosis [89–91], and complex signal transduction occurs [92]. In osteoblasts, ruffles were observed after exposure to parathyroid extract [93] and after internalization of polymer or metal particles [94]. Therefore, our present observation of PLC enzymes in membrane ruffles might be related to the effects of PLCs upon PIP2 levels.

Selected PLC enzymes were described to act during membrane ruffles formation. The involvement of PLC γ1 was described in membrane ruffles, as down-regulation of the enzyme induced marked reduction of the number of membrane ruffles [95]. In human breast cancer MDA-MB-231 cell line, PLC γ1 seems to regulate the formation of membrane ruffles and the activity of Rac [96], which once activated, induces membrane ruffles, focal adhesion complexes and lamellipodia formation [97]. PLC γ1 regulates Rac1 activation in breast cancer cells [98], probably representing the link between PI3K and Rac activity. A role of Rac activation and metastatic potential of a panel of cell variants

derived from MDA-MB-435 cell line was reported [99]. Also, another Rac downstream effector, the Wiskott-Aldrich syndrome protein (WASP) family, crucially acts in cell migration and metastasis [100]. Authors suggested that PLC γ1 probably regulates actin cytoskeleton reorganization through Rac and WASP family proteins. In our present experiments, PLC γ1 was slightly detected in untreated hOBs and until day 2 in all the experimental conditions, and it was exclusively detected in the nucleus in DMSO treated hOBs. PLC γ1 was not detected in membrane ruffles or cell protrusions. That observation might be explained with the strict cyto-specificity of PLC enzymes are, which probably bear different functions depending on the cell type and on the related signal transduction pathways, including the GTPase signaling. PLC β2 was involved in the preassembling of δ-Opioid receptor 1 DORs in Large dense-core vesicles (LDCVs) with Gαi2 and Gβ1γ5 subunits. LDCVs serve as subcellular compartments that enable activity-dependent modulation of cell membrane properties [101]. PLC β2 and PLC β3 share the possibility to be activated by Rac GTPases. The Rac1, Rac2 and Cdc42 small G proteins are direct activators of PLC β2 and, to a lesser extent, of PLC β3 [102–104].

Following the observation of a peculiar distribution of some PLC enzymes within the cell, we hypothesized that they could locate in the ER. Interestingly, co-localization experiments with the ER marker Calnexin demonstrated that PLC β1, PLC γ2, enzymes belonging to the PLC δ family and PLC ε do actually localize in the ER (Table 3, Figure 4). The ER is a major site of protein synthesis and transport, protein folding, lipid and steroid synthesis, carbohydrate metabolism and calcium storage [105–111]. The ER is composed of different domains, bearing one or more specific functions. The organization of these structural/functional subdomains is not clear. The ER is the site of protein synthesis for secreted and/or integral membrane proteins [112] and cytosolic proteins [105]. The ER is the site of bulk membrane lipid biogenesis [110] occurring in the endomembrane compartment and including the ER itself and the Golgi apparatus. Protein and phospholipid major membranes' lipid components are transferred and modified in the ER-Golgi intermediate compartment (ERGIC) region, the side of the ER juxtaposed to the Golgi apparatus rich in tubules and vesicles [113]. After mobilization to the ERGIC, lipids are conveyed throughout the cell by means of organelle contacts or secretory vesicles [114].

In addition to its role in synthesis/transport of biomolecules and lipid biogenesis, the ER is a store of intracellular calcium [115,116]. The concentration of calcium in the ER lumen is usually higher than in the cytoplasm and lower than in the extracellular compartment [108,117]. In the ER, several calcium channels, ryanodine receptors and inositol IP3 receptors (IP3R) were described that allow calcium release into the cytosol when intracellular levels are low [108]. The release of calcium follows PLC stimulation, evoked by several external stimuli, including G protein-coupled receptor (GPCR) activation [118]. PLC was demonstrated to be crucial in the stress response of the ER in Arabidopsis [119]. The presence of PLCs in the ER might be related to a stage of their synthesis. However, it is surprising that only selected PLCs were localized, and, as far as one can see, the presence might be related to cell metabolic needs. That might partially explain the presence of PLCs in the ER, but further studies are required to explain the meaning of the presence of selected PLCs.

5. Conclusions

Our results confirm that DMSO and low-dose U-73122 did not affect cell growth and survival of hOBs. We also confirm that all *PLC* genes are transcribed in hOBs and the possible transcription of splicing variants of selected *PLC* genes, depending upon the culture conditions. Quantitative analyses of PLC transcripts will be required in order to confirm variations in mRNA concentrations depending

on U-73122 treatment.

Although U-73122 had no ON/OFF effect upon the transcription of *PLC* genes, it affected the localization of PLC enzymes, supporting the hypothesis that a nuclear cycle might exist for PLC enzymes other than the PLC β1 nuclear cycle. Our data confirm the absence of PLC δ3 enzyme in quiescent hOBs at seeding. Our present results confirm the presence of selected PLC enzymes in intracellular vesicles (IVs), especially in cells cultured in the presence of DMSO.

We detected PLC enzymes in cell protrusions or pseudopodia-like structures, as previously described [12]. Moreover, we detected selected PLC enzymes in the nuclear or the plasma membrane and in membrane ruffles, suggesting involvement of PLC enzymes in EV formation or in cell movement.

We here demonstrated that selected PLC enzymes localize in the ER, slightly differing depending on the culture conditions, suggesting that probably the presence is not related exclusively to the PLC synthesis.

Further studies will be required in order to evaluate the double transcript sequence of selected PLCs, the role of PLCs in pseudopodia-like structures and membrane ruffles formation and the meaning of the presence of PLCs in the ER. Further studies about the signal transduction of PLC enzymes will offer insights into the PLC-related calcium metabolism in osteoblasts. Better knowledge of the calcium metabolism is of great interest due to the main role in bone remodeling during both growth and fractures, as well as in the progressive bone mineral reduction observed in osteopenia and osteoporosis. Insights into the calcium-related signal transduction pathways might open the way to the identification of new molecular targets for the therapeutic approach.

Acknowledgments

Conflict of interest

All authors declare no conflicts of interest in this paper.

Author contribution

Matteo Corradini: formal analysis, methodology. Marta Checchi: methodology. Carla Palumbo: conceptualization, funding acquisition. Vincenza R. Lo Vasco: conceptualization, project administration, supervision, funding acquisition, writing.

References

1. Sharma A, Sharma L, Goyal R (2021) Molecular signaling pathways and essential metabolic elements in bone remodeling: An implication of therapeutic targets for bone diseases. *Curr Drug Targets* 22: 77–104. https://doi.org/10.2174/1389450121666200910160404
2. Zaidi M (2007) Skeletal remodeling in health and disease. *Nat Med* 13: 791–801. https://doi.org/10.1038/nm1593

3. Khosla S, Riggs BL (2005) Pathophysiology of age-related bone loss and osteoporosis. E*ndocrin Metab Clin North Am* 34: 1015–1030. https://doi.org/10.1016/j.ecl.2005.07.009

4. Marie PJ (2015) Osteoblast dysfunctions in bone diseases: from cellular and molecular mechanisms to therapeutic strategies. *Cell Mol Life Sci* 72: 1347–1361. https://doi.org/10.1007/s00018-014-1801-2

5. Kawai M, Modder UI, Khosla S, et al. (2011) Emerging therapeutic opportunities for skeletal restoration. *Nat Rev Drug Discov* 10: 141–156. https://doi.org/10.1038/nrd3299

6. Gether U (2000) Uncovering molecular mechanisms involved in activation of G protein-coupled receptors. *Endocr Rev* 21: 90–113. https://doi.org/10.1210/edrv.21.1.0390

7. Wu M, Deng L, Zhu G, et al. (2010) G Protein and its signaling pathway in bone development and disease. *Front Biosci (Landmark Ed)* 15: 957–985. https://doi.org/10.2741/3656

8. Bowler WB, Gallagher JA, Bilbe G (1998) G-protein coupled receptors in bone. *Front Biosci* 3: 769–780. https://doi.org/10.2741/a320

9. Conklin BR, Hsiao EC, Claeysen S, et al. (2008) Engineering GPCR signaling pathways with RASSLs. *Nat Methods* 5: 673–678. https://doi.org/10.1038/nmeth.1232

10. Saggio I, Remoli C, Spica E, et al. (2014) Constitutive expression of Gsα(R201C) in mice produces a heriTable, direct replica of human fibrous dysplasia bone pathology and demonstrates its natural history. *J Bone Miner Res* 29: 2357–2368. https://doi.org/10.1002/jbmr.2267

11. Remoli C, Michienzi S, Sacchetti B, et al. (2015) Osteoblast-specific expression of the fibrous dysplasia (FD)-causing mutation Gsα(R201C) produces a high bone mass phenotype but does not reproduce FD in the mouse. *J Bone Miner Res* 30: 1030–1043. https://doi.org/10.1002/jbmr.2425

12. Daisy CS, Romanelli A, Checchi M, et al. (2022) Expression and localization of Phosphoinositide-specific Phospholipases C in cultured, differentiating and stimulated human osteoblasts. *J Cell Signal* 3: 44–61. https://doi.org/10.33696/Signaling.3.067

13. Berridge MJ, Irvine RF (1984) Inositol triphosphate, a novel second messenger in cellular signal transduction. *Nature* 312: 315–321. https://doi.org/10.1038/312315a0

14. Berridge MJ (1981) Phosphatidylinositol hydrolysis: a multifunctional transducing mechanism. *Mol Cell Endocrinol* 24: 115–140. https://doi.org/10.1016/0303-7207(81)90055-1

15. Berridge MJ (2009) Inositol trisphosphate and calcium signalling mechanisms. *Biochim Biophys Acta* 1793: 933–940. https://doi.org/10.1016/j.bbamcr.2008.10.005

16. Tang X, Edwards EM, Holmes BB, et al. (2006) Role of phospholipase C and diacylglyceride lipase pathway in arachidonic acid release and acetylcholine-induced vascular relaxation in rabbit aorta. *Am J Physiol Heart Circ Physiol* 290: H37–H45. https://doi.org/10.1152/ajpheart.00491.2005

17. Suh PG, Park J, Manzoli L, et al. (2008) Multiple roles of phosphoinositide-specific phospholipase C isozymes. *BMB Rep* 41: 415–434. https://doi.org/10.5483/bmbrep.2008.41.6.415

18. Mebarek S, Abousalham A, Magne D, et al. (2013) Phospholipases of mineralization competent cells and matrix vesicles: roles in physiological and pathological mineralizations. *Int J Mol Sci* 14: 5036–5129. https://doi.org/10.3390/ijms14035036

19. Bahk YY, Song H, Baek SH, et al. (1998) Localization of two forms of phospholipase C-beta1, a and b, in C6Bu-1 cells. *Biochim Biophys Acta* 1389: 76–80. https://doi.org/10.1016/S0005-2760(97)00128-8

20. Mao GF, Kunapuli SP, Koneti Rao A (2000) Evidence for two alternatively spliced forms of phospholipase C-beta2 in haematopoietic cells. *Brit J Haematol* 110: 402–408. https://doi.org/10.1046/j.1365-2141.2000.02201.x

21. Kim MJ, Min DS, Ryu SH, et al. (1998) A cytosolic, galphaq- and betagamma-insensitive splice variant of phospholipase C-beta4. *J Biol Chem* 273: 3618–3624. https://doi.org/10.1074/jbc.273.6.3618

22. Lee SB, Rhee SG (1996) Molecular cloning, splice variants, expression, and purification of phospholipase C-delta 4. *J Biol Chem* 271: 25–31. https://doi.org/10.1074/jbc.271.1.25

23. Sorli SC, Bunney TD, Sugden PH, et al. (2005) Signaling properties and expression in normal and tumor tissues of two phospholipase C epsilon splice variants. *Oncogene* 24: 90–100. https://doi.org/10.1038/sj.onc.1208168

24. Lo Vasco VR, Fabrizi C, Artico M, et al. (2007) Expression of phosphoinositide-specific phospholipase C isoenzymes in cultured astrocytes. *J Cell Biochem* 100: 952–959. https://doi.org/10.1002/jcb.21048

25. Lo Vasco VR, Pacini L, Di Raimo T (2011) Expression of phosphoinositide-specific phospholipase C isoforms in human umbilical vein endothelial cells. *J Clin Pathol* 64: 911–915. http://dx.doi.org/10.1136/jclinpath-2011-200096

26. Lo Vasco VR, Leopizzi M, Chiappetta C, et al. (2012) Expression of Phosphoinositide-specific Phospholipase C enzymes in normal endometrium and in endometriosis. *Fertil Steril* 98: 410–414. https://doi.org/10.1016/j.fertnstert.2012.04.020

27. Lo Vasco VR, Leopizzi M, Chiappetta C, et al. (2013) Expression of Phosphoinositide-specific phospholipase C enzymes in human osteosarcoma cell lines. *J Cell Commun Signal* 7: 141–150. https://doi.org/10.1007/s12079-013-0194-6

28. Fais P, Leopizzi M, Di Maio V, et al. (2019) Phosphoinositide-specific Phospholipase C in normal human liver and in alcohol abuse. *J Cell Biochem* 120: 7907–7917. https://doi.org/10.1002/jcb.28067

29. Leopizzi M, Di Maio V, Della Rocca C, et al. (2020) Supernatants from human osteosarcoma cultured cell lines induce modifications in growth and differentiation of THP-1 cells and phosphoinositide-specific phospholipase C enzymes. *Multidiscip Cancer Invest* 4: 1–12. https://doi.org/10.30699/mci.4.4.430

30. Hwang JI, Kim HS, Lee JR, et al. (2005) The interaction of phospholipase C-beta3 with Shank2 regulates mGluR-mediated calcium signal. *J Biol Chem* 280: 12467–12473. https://doi.org/10.1074/jbc.M410740200

31. Bertagnolo V, Mazzoni M, Ricci D, et al. (1995) Identification of PI-PLC beta 1, gamma 1, and delta 1 in rat liver: subcellular distribution and relationship to inositol lipid nuclear signalling. *Cell Signal* 7: 669–678. https://doi.org/10.1016/0898-6568(95)00036-O

32. Nishida T, Huang TP, Seiyama A, et al. (1998) Endothelin A-receptor blockade worsens endotoxin-induced hepatic microcirculatory changes and necrosis. *Gastroenterology* 115: 412–420. https://doi.org/10.1016/s0016-5085(98)70208-2

33. Lo Vasco VR, Fabrizi C, Fumagalli L, et al. (2010) Expression of phosphoinositide specific phospholipase C isoenzymes in cultured astrocytes activated after stimulation with Lipopolysaccharide. *J Cell Biochem* 109: 1006–1012. https://doi.org/10.1002/jcb.22480

34. Lo Vasco VR, Leopizzi M, Chiappetta C, et al. (2013) Lypopolysaccharide down-regulates the expression of selected phospholipase C genes in cultured endothelial cells. *Inflammation* 36: 862–868. https://doi.org/10.1007/s10753-013-9613-3

35. Lo Vasco VR, Leopizzi M, Puggioni C, et al. (2014) Neuropeptide Y significantly reduces the expression of PLCB2, PLCD1 and moderately decreases selected PLC genes in endothelial cells. *Mol Cell Biochem* 394: 43–52. https://doi.org/10.1007/s11010-014-2079-2

36. Lo Vasco VR, Leopizzi M, Puggioni C, et al. (2014) Fibroblast growth factor acts upon the transcription of phospholipase C genes in human umbilical vein endothelial cells. *Mol Cell Biochem* 388: 51–59. https://doi.org/10.1007/s11010-013-1898-x

37. Di Raimo T, Leopizzi M, Mangino G, et al. (2016) Different expression and subcellular localization of Phosphoinositide-specific Phospholipase C enzymes in differently polarized macrophages. *J Cell Commun Signal* 10: 283–293. https://doi.org/0.1007/s12079-016-0335-9

38. Lo Vasco VR, Fabrizi C, Panetta B, et al. (2010) Expression pattern and sub cellular distribution of Phosphoinositide specific Phospholipase C enzymes after treatment with U-73122 in rat astrocytoma cells. *J Cell Biochem* 110: 1005–1012. https://doi.org/10.1002/jcb.22614

39. Lo Vasco VR, Leopizzi M, Di Maio V, et al. (2016) U-73122 reduces the cell growth in cultured MG-63 ostesarcoma cell line involving Phosphoinositide-specific Phospholipases C. *Springerplus* 5: 156. https://doi.org/10.1186/s40064-016-1768-6

40. Lo Vasco VR (2010) Signalling in the genomic era. *J Cell Commun Signal* 4: 115–117. https://doi.org/10.1007/s12079-010-0091-1

41. Urciuoli E, Leopizzi M, Di Maio V, et al. (2020) Phosphoinositide-specific phospholipase C isoforms are conveyed by osteosarcoma-derived extracellular vesicles. *J Cell Commun Signal* 14: 417–426. https://doi.org/10.1007/s12079-020-00571-6

42. Bleasdale JE, Thakur NR, Gremban RS, et al. (1990) Selective inhibition of receptor-coupled phospholipase C dependent processes in human platelets and polymorphonuclear neutrophils. *J Pharmacol Exp Ther* 255:756–768.

43. Hellberg C, Molony L, Zheng L, et al. (1996) Ca^{2+} signalling mechanisms of the β2 integrin on neutrophils: involvement of phospholipase Cγ2 and Ins (1, 4, 5) P3. *Biochem J* 317: 403–409. https://doi.org/10.1042/bj3170403

44. Smallridge RC, Kiang JG, Gist ID, et al. (1992) U-73122, an aminosteroid phospholipase C antagonist, non-competitively inhibits thyrotropin-releasing hormone effects in GH3 rat pituitary cells. *Endocrinology* 131: 1883–1888. https://doi.org/10.1210/endo.131.4.1396332

45. Yang YR, Follo MY, Cocco L, et al. (2013) The physiological roles of primary phospholipase C. *Adv Biol Regul* 53: 232–241. https://doi.org/10.1016/j.jbior.2013.08.003

46. Ramazzotti G, Bavelloni A, Blalock W, et al. (2016) BMP-2 Induced Expression of PLCβ1 That is a Positive Regulator of Osteoblast Differentiation. *J Cell Physiol* 231: 623–629. https://doi.org/10.1002/jcp.25107

47. Rammler DH, Zaffaroni A (1967) Biological implications of DMSO based on a review of its chemical properties. *Ann N Y Acad Sci* 141: 13–23. https://doi.org/10.1111/j.1749-6632.1967.tb34861.x

48. Jacob SW, Herschler R (1986) Pharmacology of DMSO. *Cryobiology* 23: 14–27. https://doi.org/10.1016/0011-2240(86)90014-3

49. Li X, Majdi S, Dunevall J, et al. (2015) Quantitative measurement of transmitters in individual vesicles in the cytoplasm of single cells with nanotip electrodes. *Angew Chem Int Ed Engl* 54: 11978–11982. https://doi.org/10.1002/anie.201504839

50. Norwood TH, Zeigler CJ, Martin GM (1976) Dimethyl sulfoxide enhances polyethylene glycol-mediated somatic cell fusion. *Somatic Cell Genet* 2: 263–270. https://doi.org/10.1007/bf01538964

51. Norwood TH, Zeigler CJ (1982) The use of dimethyl sulfoxide in mammalian cell fusion, *Techniques in Somatic Cell Genetics*, Boston: Springer. https://doi.org/10.1007/978-1-4684-4271-7_4

52. Santos NC, Figueira-Coelho J, Martins-Silva J, et al. (2003) Multidisciplinary utilization of dimethyl sulfoxide: pharmacological, cellular, and molecular aspects. *Biochem Pharmacol* 65: 1035–1041. https://doi.org/10.1016/s0006-2952(03)00002-9

53. Spray DC, Campos de Carvalho AC, Mendez-Otero R (2010) Chemical induction of cardiac differentiation in p19 embryonal carcinoma stem cells. *Stem Cells Dev* 19: 403–412. https://doi.org/10.1089/scd.2009.0234

54. Galvao J, Davis B, Tilley M (2013) Unexpected low-dose toxicity of the universal solvent DMSO. *FASEB J* 28: 1317–1330. https://doi.org/10.1096/fj.13-235440

55. Best BP (2015) Cryoprotectant toxicity: facts, issues, and questions. *Rejuvenation Res* 18: 422–36. https://doi.org/10.1089/rej.2014.1656

56. Majdi S, Najafinobar N, Dunevall J, et al. (2017) DMSO chemically alters cell membranes to slow exocytosis and increase the fraction of partial transmitter released. *Chembiochem* 18: 1898–1902. https://doi.org/10.1002/cbic.201700410

57. de Ménorval MA, Mir LM, Fernández ML, et al. (2012) Effects of dimethyl sulfoxide in cholesterol-containing lipid membranes: a comparative study of experiments in silico and with cells. *PLoS One* 7: e41733. https://doi.org/10.1371/journal.pone.0041733

58. Notman R, Noro M, O'Malley B, et al. (2006) Molecular basis for dimethylsulfoxide (DMSO) action on lipid membranes. *J Am Chem Soc* 128: 13982–13983. https://doi.org/10.1021/ja063363t

59. Gurtovenko AA, Anwar J (2007) Modulating the structure and properties of cell membranes: the molecular mechanism of action of dimethyl sulfoxide. *J Phys Chem B* 111: 10453–10460. https://doi.org/10.1021/jp073113e

60. Hughes ZE, Mark AE, Mancera RL (2012) Molecular dynamics simulations of the interactions of DMSO with DPPC and DOPC phospholipid membranes. *J Phys Chem B* 116: 11911–11923. https://doi.org/10.1021/jp3035538

61. Gironi B, Kahveci Z, McGill B, et al. (2020) Effect of DMSO on the mechanical and structural properties of mmodel and biological mmembranes. *Biophys J* 119: 274–286. https://doi.org/10.1016/j.bpj.2020.05.037

62. Vickers AE, Fisher RL (2004) Organ slices for the evaluation of human drug toxicity. *Chem Biol Interact* 150: 87–96. https://doi.org/10.1016/j.cbi.2004.09.005

63. Thomas MJ, Smith A, Head DH, et al. (2005) Airway inflammation: chemokine-induced neutrophilia and the class I phosphoinositide 3-kinases. *Eur J Immunol* 35: 1283–1291. https://doi.org/10.1002/eji.200425634

64. Cenni B, Picard D (1999) Two compounds commonly used for phospholipase C inhibition activate the nuclear estrogen receptors. *Biochem Biophys Res Commun* 261: 340–344. https://doi.org/10.1006/bbrc.1999.1017

65. Feisst C, Albert D, Steinhilber D, et al. (2005) The aminosteroid phospholipase C antagonist U-73122 (1-[6-[[17-beta-3-methoxyestra-1,3,5(10)-trien-17-yl]amino]hexyl]-1Hpyrrole-2,5-dione) potently inhibits human 5-lipoxygenase in vivo and in vitro. *Mol Pharmacol* 67: 1751–1757. https://doi.org/10.1124/mol.105.011007

66. Hughes S, Gibson WJ, Young JM (2000) The interaction of U-73122 with the histamine H-1 receptor: implications for the use of U-73122 in defining H-1 receptor-coupled signalling pathways. *Naunyn Schmiedeberg's Arch Pharmacol* 362: 555–558. https://doi.org/10.1007/s002100000326

67. Walker EM, Bispham JR, Hill SJ (1998) Nonselective effects of the putative phospholipase C inhibitor, U73122, on adenosine A(1) receptor-mediated signal transduction events in Chinese hamster ovary cells. *Biochem Pharmacol* 56: 1455–1462. https://doi.org/10.1016/s0006-2952(98)00256-1

68. Berven LA, Barritt GJ (1995) Evidence obtained using single hepatocytes for inhibition by the phospholipase-C inhibitor U73122 of store-operated Ca^{2+} inflow. *Biochem Pharmacol* 49: 1373–1379. https://doi.org/10.1016/0006-2952(95)00050-a

69. Pulcinelli FM, Gresele P, Bonuglia M, et al. (1998) Evidence for separate effects of U73122 on phospholipase C and calcium channels in human platelets. *Biochem Pharmacol* 56: 1481–1484. https://doi.org/10.1016/s0006-2952(98)00146-4

70. Boujard D, Anselme B, Cullin C, et al. (2014) Vesikulärer Transport. In Boujard, D.B., Anselme, C., Cullin, C., Raguenes, Nicol., *Zell- und Molekularbiologie im Überblick*, Berlin: Springer Spektrum. https://doi.org/10.1007/978-3-642-41761-0

71. Bray D (1992) *Cell Movements: From Molecules to Motility.* New York: Garland Publishing Inc. https://doi.org/10.4324/9780203833582

72. Chhabra ES, Higgs HN (2007) The many faces of actin: matching assembly factors with cellular structures. *Nat Cell Biol* 9: 1110–1121. https://doi.org/10.1038/ncb1007-1110

73. Lauffenburger DA, Horwitz FA (1996) Cell migration: a physically integrated molecular process. *Cell* 84: 359–369. https://doi.org/10.1016/s0092-8674(00)81280-5

74. Ridley AJ, Schwartz MA, Burridge K, et al. (2003) Cell migration: integrating signals from front to back. *Science* 302: 1704–1709. https://doi.org/10.1126/science.1092053

75. Pollard TD, Borisy GG (2003) Cellular motility driven by assembly and disassembly of actin filaments. *Cell* 112: 453– 465. https://doi.org/10.1016/s0092-8674(03)00120-x

76. Chan AY, Raft S, Bailly M, et al. (1998) EGF stimulates an increase in actin nucleation and filament number at the leading edge of the lamellipod in mammary adenocarcinoma cells. *J Cell Sci* 111: 199–211. https://doi.org/10.1242/jcs.111.2.199

77. Damsky CH, Ilić D (2002) Integrin signaling: it's where the action is. *Curr Opin Cell Biol* 14: 594–602. https://doi.org/10.1016/s0955-0674(02)00368-x

78. Hynes RO (2002) Integrins: bidirectional, allosteric signaling machines. *Cell* 110: 673–687. https://doi.org/10.1016/s0092-8674(02)00971-6

79. Wells A (1999) EGF receptor. *Int J Biochem Cell Biol* 31: 637–643. https://doi.org/10.1016/s1357-2725(99)00015-1

80. DeMali KA, Wennerberg K, Burridge K (2003) Integrin signaling to the actin cytoskeleton. *Curr Opin Cell Biol* 15: 572–582. https://doi.org/10.1016/s0955-0674(03)00109-1

81. Aspenström P (1999) Effectors for the Rho GTPases. *Curr Opin Cell Biol* 11: 95–102. https://doi.org/10.1016/s0955-0674(99)80011-8

82. DeMali KA, Burridge K (2003) Coupling membrane protrusion and cell adhesion. *J Cell Sci* 116: 2389–2397. https://doi.org/10.1242/jcs.00605

83. Burridge K, Wennerberg K (2004) Rho and Rac take center stage. *Cell* 116: 167–179. https://doi.org/10.1016/s0092-8674(04)00003-0

84. Beningo KA, Dembo M, Kaverina I, et al. (2001) Nascent focal adhesions are responsible for the generation of strong propulsive forces in migrating fibroblasts. *J Cell Biol* 153: 881–888. https://doi.org/10.1083/jcb.153.4.881

85. Balaban NQ, Schwarz US, Riveline D, et al. (2001) Force and focal adhesion assembly: a close relationship studied using elastic micropatterned substrates. *Nat Cell Biol* 3: 466–472. https://doi.org/10.1038/35074532

86. Abercrombie M (1980) The Croonian Lecture, 1978-The crawling movement of metazoan cells. *Proc R Soc Lond, Ser B* 207: 129–147. https://doi.org/10.1098/rspb.1980.0017

87. Hinz B, Alt W, Johnen C, et al. (1999) Quantifying lamella dynamics of cultured cells by SACED, a new computer-assisted motion analysis. *Exp Cell Res* 251: 234–243. https://doi.org/10.1006/excr.1999.4541

88. Araki N, Egami Y, Watanabe Y, et al. (2007) Phosphoinositide metabolism during membrane ruffling and macropinosome formation in EGF-stimulated A431 cells. *Exp Cell Res* 313: 1496–1507. https://doi.org/10.1016/j.yexcr.2007.02.012

89. Rilla K, Koistinen A (2015) Correlative light and electron microscopy reveals the HAS3-induced dorsal plasma membrane ruffles. *Int J Cell Biol* 2015: 769163. https://doi.org/10.1155/2015/769163

90. Hoon JL, Wong WK, Koh CG (2012) Functions and regulation of circular dorsal ruffles. *Mol Cell Biol* 32: 4246–4257. https://doi.org/10.1128/MCB.00551-12

91. Bernitt E, Döbereiner HG, Gov NS, et al. (2017) Fronts and waves of actin polymerization in a bistability-based mechanism of circular dorsal ruffles. *Nat Commun* 8: 15863. https://doi.org/10.1038/ncomms15863

92. Li G, D'Souza-Schorey C, Barbieri MA, et al. (1997) Uncoupling of membrane ruffling and pinocytosis during Ras signal transduction. *J Biol Chem* 272: 10337–10340. https://doi.org/10.1074/jbc.272.16.10337

93. Jones SJ, Boyde A (1976) Morphological changes of osteoblasts in vitro. *Cell Tissue Res* 166: 101–107. https://doi.org/10.1007/BF00215129

94. Lohmann CH, Schwartz Z, Köster G, et al. (2000) Phagocytosis of wear debris by osteoblasts affects differentiation and local factor production in a manner dependent on particle composition. *Biomaterials* 21: 551–561. https://doi.org/10.1016/s0142-9612(99)00211-2

95. Sala G, Dituri F, Raimondi C, et al. (2008) PPhospholipase Cγ1 is required for metastasis development and progression. *Cancer Res* 68: 10187–10196. https://doi.org/10.1158/0008-5472.CAN-08-1181

96. Barber MA, Welch HCE (2006) PI3K and RAC signaling in leukocyte and cancer cell migration. *Bull Cancer* 93: 10044–10052.

97. Marée, AF, Grieneisen VA, Edelstein-Keshet L (2012) How cells integrate complex stimuli: the effect of feedback from phosphoinositides and cell shape on cell polarization and motility. *PLoS computational biology* 8: e1002402. https://doi.org/10.1371/journal.pcbi.1002402

98. Razzini G, Berrie CP, Vignati S, et al. (2000) Novel functional PI 3-kinase antagonists inhibit cell growth and tumorigenicity in human cancer cell lines. *FASEB J* 14: 1179–1187. https://doi.org/10.1096/fasebj.14.9.1179

99. Baugher PJ, Krishnamoorthy L, Price JE (2005) Rac1 and Rac3 isoform activation is involved in the invasive and metastatic phenotype of human breast cancer cells. *Breast Cancer Res* 7: R965–R974. https://doi.org/10.1186/bcr1329

100. Takenawa T, Miki H (2001) WASP and WAVE family proteins: key molecules for rapid rearrangement of cortical actin filaments and cell movement. *J Cell Sci* 114: 1801–1809. https://doi.org/10.1242/jcs.114.10.1801

101. Zhao B, Wang HB, Lu YJ, et al. (2011) Transport of receptors, receptor signaling complexes and ion channels via neuropeptide-secretory vesicles. *Cell Res* 21: 741–753. https://doi.org/10.1038/cr.2011.29

102. Illenberger D, Schwald F, Gierschik P (1997) Characterization and purification from bovine neutrophils of a soluble guanine-nucleotide-binding protein that mediates isozyme-specific stimulation of phospholipase C beta2. *Eur J Biochem* 246: 71–77. https://doi.org/10.1111/j.1432-1033.1997.t01-1-00071.x

103. Illenberger D, Schwald F, Pimmer D, et al. (1998) Stimulation of phospholipase C-β2 by the Rho GTPases Cdc42Hs and Rac1. *EMBO J* 17: 6241–6249. https://doi.org/10.1093/emboj/17.21.6241

104. Illenberger D, Walliser C, Strobel J, et al. (2003) Rac2 regulation of phospholipase C-β 2 activity and mode of membrane interactions in intact cells. *J Biol Chem* 278: 8645–8652. https://doi.org/10.1074/jbc.m211971200

105. Reid DW, Nicchitta CV (2015) Diversity and selectivity in mRNA translation on the endoplasmic reticulum. *Nat Rev Mol Cell Biol* 16: 221–231. https://doi.org/10.1038/nrm3958

106. Rapoport TA (2007) Protein translocation across the eukaryotic endoplasmic reticulum and bacterial plasma membranes. *Nature* 450: 663–669. https://doi.org/10.1038/nature06384

107. Braakman I, Hebert DN (2013) Protein folding in the endoplasmic reticulum. *Cold Spring Harb Perspect Biol* 5: a013201. https://doi.org/10.1101/cshperspect.a013201

108. Fagone P, Jackowski S (2009) Membrane phospholipid synthesis and endoplasmic reticulum function. *J Lipid Res* 50: S311–S316. https://doi.org/10.1194/jlr.R800049-JLR200

109. Hebert DN, Garman SC, Molinari M (2005) The glycan code of the endoplasmic reticulum: asparagine-linked carbohydrates as protein maturation and quality-control tags. *Trends Cell Biol* 15: 364–370. https://doi.org/10.1016/j.tcb.2005.05.007

110. Clapham DE (2007) Calcium signaling. *Cell* 131: 1047–1058. https://doi.org/10.1016/j.cell.2007.11.028

111. Westrate LM, Lee JE, Prinz WA, et al. (2015) Form follows function: the importance of endoplasmic reticulum shape. *Annu Rev Biochem* 84: 791–811. https://doi.org/10.1146/annurev-biochem-072711-163501

112. Jan CH, Williams CC, Weissman JS (2014) Principles of ER cotranslational translocation revealed by proximity-specific ribosome profiling. *Science* 346: 1257521. https://doi.org/10.1126/science.1257521

113. Glick BS, Nakano A (2009) Membrane traffic within the Golgi apparatus. *Annu Rev Cell Dev Biol* 25: 113–132. https://doi.org/10.1146/annurev.cellbio.24.110707.175421

114. Appenzeller-Herzog C, Hauri HP (2006) The ER-Golgi intermediate compartment (ERGIC): in search of its identity and function. *J Cell Sci* 119: 2173–2183. https://doi.org/10.1242/jcs.03019

115. Jaffe LF (1983) Sources of calcium in egg activation: a review and hypothesis. *Dev Biol* 99: 265–276. https://doi.org/10.1016/0012-1606(83)90276-2

116. Eisen A, Reynolds GT (1985) Source and sinks for the calcium released during fertilization of single sea urchin eggs. *J Cell Biol* 100: 1522–1527. https://doi.org/10.1083/jcb.100.5.1522

117. Samtleben S, Jaepel J, Fecher C, et al. (2013) Direct imaging of ER calcium with targeted-esterase induced dye loading (TED). *J Vis Exp* 75: e50317. https://doi.org/10.3791/50317

118. Oude Weernink PA, Han L, Jakobs KH, et al. (2007) Dynamic phospholipid signaling by G protein-coupled receptors. *Biochim Biophys Acta* 1768: 888–900. https://doi.org/10.1016/j.bbamem.2006.09.012

119. Kanehara K, Yu CY, Cho Y, et al. (2015) Arabidopsis AtPLC2 is a primary phosphoinositide-specific phospholipase C in phosphoinositide metabolism and the endoplasmic reticulum stress response. *PLoS Genet* 11: e1005511. https://doi.org/10.1371/journal.pgen.1005511